A Hybrid Combining Hard and Soft Robots

Adam A. Stokes, Robert F. Shepherd, Stephen A. Morin, Filip Ilievski, and George M. Whitesides*

SUPPLEMENTAL INFORMATION

Department of Chemistry and Chemical Biology, Harvard University

12 Oxford Street, Cambridge, MA 02138

*Corresponding author, email: gwhitesides@gmwgroup.harvard.edu

Multimedia

Video S1: Retrieval of an object by the hybrid system

Video S2: Gripping of a lightbulb by the soft robot

Video S3: Directional control of the robot

Video S4: Motion capture analysis of the soft robot walking on a flat surface

Video S5: The soft robot walking on sand

Video S6: Motion capture analysis of the soft robot walking on sand

Video S7: The soft robot climbing an inclined surface

Technical Files

SI PCB CAD Files.zip contains:

The PCB gerber files.

The laser cutting CAD files for the microcompressor/valve mounting racks.

The bill of materials for the electronics components required to populate the PCB.

The source code.

Supplemental Design Details

S1.1 Design of the soft robotic sub-system

Our legged design allows us to drive the robot over sand, and up inclines. For actuation, we incorporated a double pneu-net structure into each of the four legs. This network allowed movement in any direction across a surface. These robots used a battery-powered electro-pneumatic control system that included valves and pumps taken from low-cost (~$10), commercial blood-pressure monitors used for home health-care. We have also implemented paper-based piezo-MEMS bump sensors [8], so that the control system of the robot can alter its course autonomously based on feedback from its environment. An alternative type of soft sensor has been developed by Kramer and Majidi et al.[26-28]; it uses liquid metal alloy networks, embedded in elastomers; this sensing mechanism could be used in future designs of soft robots.

The soft robot we describe here is inexpensive, versatile, and autonomous. Although still tethered, this design has two important advantages useful in exploring unstable terrain; the tethers allow: i) heavy and more expensive components to remain off-board and ii) the possibility of transferring liquids/gases/foams/granules from a remote location along the tether, and to or from the soft robot. The capability of mass transport has been used by Morin et al. [4] to camouflage or display a soft robot, and by Martinez et al. [29] to move acid, sand, and salt using a tentacle-like fluidic system.

S1.2. Design of the quadruped

We designed a quadrupedal soft robot that can be steered in four directions. It is 15 cm in length, measured diagonally across its center (Figure S2). The robot contains two parallel pneu-nets in each of the four legs; these pneu-nets run from the center of the body to the tip of the leg. The parallel pneu-nets allow us to actuate each leg in a "paddling" motion using three steps (Figure S3a-d): i) both pneu-nets are, initially, at atmospheric pressure; ii) the tip of the leg moves forward-and-down by inflating pneu-net 1; iii) the same tip then moves down-and-back by inflating both pneu-nets; iv) it then moves upward-and-backwards by deflating pneu-net 2; v) the leg returns to its initial position by deflating both pneu-nets. The actuation/deactuation sequence of each of the four legs determines the direction of the robot.

The robot is C4 rotationally symmetric. Interestingly, nature rarely adopts this body plan: it is found only in certain jellyfish and some plants.[2] We chose this design because it allows the robot to move across a surface in four directions of travel, and the symmetry simplifies the design of the control system. The symmetric design eliminates the need for the robot to turn-in-place (as for other quadrupedal[30] and wheeled or tracked robots[5])—the control system simply redefines which side of the robot is now acting as the "front."

S1.3. Design of the pneumatic control system

We designed the printed circuit board (PCB) for the controller in-house, and it was fabricated by a commercial vendor (my4pcb.com.) The PCB provides the circuitry to run the microcompressors and valves (both sourced from commercial sphygmomanometers: $12 for one valve and one pump.) We programmed a microcontroller (Arduino Mega2560, DigiKey # 1050-1018-ND) to provide the control signals

S1.4. Design of the actuation sequence

Since the robot is rotationally symmetric, it has no front, back, or side. The gait of the robot is controlled by the direction of paddle of each leg, and the timing offset between the actuation of each leg. The gait we employ is similar to that used by tortoises and other slow-moving quadrupedal animals[31]; Figure S6.

S1.5. Design of the paper-based bump sensors for feedback

For these robots to operate in terrain more complex than an open, flat surface, they must be able to sense their surroundings. For closed-loop feedback in the robotic system, we chose paper-based piezoresistive MEMS sensors[20, 21] because they are inexpensive and easy to fabricate. The sensors allowed the control system to adapt the direction of locomotion of the robot to the presence of obstacles. For example, if the sensor touched an obstacle such as a wall, the control system could respond by reversing the direction of locomotion to avoid contact with the object before trying a new direction. We designed a sensor network that comprises a four-armed paper origami structure. Each sensor arm has, at its tip, a flexible hinge that is patterned with carbon ink via stenciling to form a bump sensor. Bending one of the flexible paper structures leads to a change in resistance of the piezoresistive carbon sensor. We threshold the output from each sensor, as it is read by the analog to digital (ADC) converter in the microcontroller, to give a binary (on/off) input to the control software.

Using a die-cutting machine (Silhouette Cameo) we created a system of paper origami-carbon ink bump sensors on Whatman 3MM chromatography paper, 340 µm thick, 186 gm-2.
We designed the net to fold up along perforated lines into triangular tube sections, for rigidity (Figure S10b). We made a stencil by laser cutting a thin acetate sheet and used carbon black ink to print four piezoresistive sensors at the hinged section of each arm (Figure S10a). Using silver epoxy, we affixed thin enameled copper wires to the sensors, and routed the wire bundle alongside the pneumatic tether to the control board (Figure S10c).

Supplemental Fabrication Details

S2.1. Fabrication of the soft robot

We fabricated the robots using soft lithography[32, 33] following protocols we have reported previously[19, 22]. We designed the tip of each leg to be rounded to allow a smooth rolling motion of the tip with the surface on which the robot is moving (Figure S2). This architecture was critical for walking on sand. We demonstrated that the quadrupedal soft robot can walk in any of four directions.
We printed ABS molds by fused deposition modeling (FDM) in a Dimension Elite 3D printer (Stratasys, Inc., Eden Prairie, MN). We mixed poly(dimethylsiloxane) (PDMS) pre-polymer (Sylgard 184, Dow) 10:1 w:w with curing agent in accordance with the manufacturer's instructions. We cast 4 mm thick sheets of PDMS on glass and cured them at 80 °C for 4 hours. We mixed the two parts of Ecoflex (Ecoflex 00-50, Smooth-On Inc.) 1:1 v:v at room temperature. We dissolved approximately 10 mg of crystal violet dye (tris(4-(dimethylamino)phenyl)methylium chloride, VWR # 101109-608) in 25 mL of dichloromethane and mixed this solution into the ecoflex silicone pre-polymer. We degassed the ecoflex/dye mixture for 5 min, poured it into the ABS mold, and then cured it at 80 °C for 20 min in a convection oven. We demolded the robot and bonded it, using PDMS pre-polymer, to the 4 mm thick PDMS sheets, we cured the robot for 24 h at room temperature. We then cut the robot from the glass and, using a cannula, we inserted silicone tubing into each pneu-net.

S2.2. Fabrication and programming of the electromechanical control system

We used a home-built control system—a printed circuit board, simple circuitry, a microcontroller, and a series of microcompressors and valves—to operate the robots. We programmed the microcontroller to execute a series of maneuvers. Figure S4 (still-frames from Video S3) shows a robot walking clockwise, in a rectilinear pattern. The robot changes direction, as described earlier, with no physical turning of the robot.

Printed circuit boards were designed in-house and manufactured by my4pcb.com. The PCB CAD files, and bill of materials for the electrical components, are provided as files. The PCB was designed to fit the popular Arduino microcontroller platform.

S2.3. Walking on sand and up an incline

We designed this robot to be light weight and to have a low center-of-gravity; these attributes enable it to traverse unstable terrain. Figure S7b shows a still frame from Video S5 of a robot walking on sand. These robots can also navigate a shallow incline. Figure S7a (a still frame from Video S7) shows a robot climbing a ramp covered with a sheet of paper. The robot is shown at its maximum climbing angle (~15°); on steeper inclines it loses traction. These demonstrations suggest possible designs for specific types of terrain.

S2.4. Acquisition of motion tracking data

To track the position of the robot, we read individual frames from Video S3 and Video S5 into Matlab ®. Firstly, we selected the blue channel from the RGB image and inverted the image intensities; the blues then became bright and the rest of the image dark. Secondly, we thresholded the image so that the only information in the image was that of the robot. Finally, we found the center of pixel intensity (i.e., the robot's center of mass) using the 'centroid' subroutine of regionprops (prepackaged code within Matlab ®) and tracked this centroid in all image frames.

We performed motion tracking analysis on the video of the directionally controlled robot (Video S4) and also on the video of the robot walking on sand (Video S6). Using the motion-tracking data, we determined that the quadrupedal soft robot is capable of walking in any of the four directions at an average speed of 6.51 m/h (~62 body lengths/hour; Video S3). Figure S5 provides the processed distance-time plots: S5a shows the X-axis location of the robot as a function of time, the origin is defined as the upper left-most corner of the frame; S5b shows the corresponding Y-axis data. We plotted linear regression lines to these data and extracted the average speed in each of the four corresponding directions shown in Figure S5: 7.2, 6.3, 5.9, and 6.7 m/h. We performed a similar analysis for the robot walking on sand (Figure S8); on this surface, the robot moves at 5.0 m/h (~50 body lengths/hour), approximately 80% of the velocity on a hard flat surface.

S2.5. Fabrication of the piezoresistive paper sensors

Using a die-cutting machine (Silhouette Cameo) we created paper origami-carbon ink bump sensors (Figure S10). The control system measures the resistance of the carbon ink in the sensors—this resistance changes as a function of the angle of flex at the hinge[21]—and uses the measurement to determine if the robot needs to change course. The bump-sensors show proof of concept in allowing the robot to move reactively—it can alter its course due to interaction with an object, such as a wall. Figure S10c shows the bump-sensor network mounted on the robot, the pneumatic tether, and the electrical tether. The total cost of the control system is approximately $150; the robot, plus sensor network, costs approximately $5.

Figure S1. A block-diagram of the distributed control system. The main program runs on an Arduino MEGA 2560 microcontroller on the electro-pneumatic control (EPC) board. The EPC uses serial communications to direct the motion of the iRobot Create©. An XBee wireless communications system runs on another Arduino microcontroller where it passes commands to and from the EPC and a remote computer. The soft robot connects to the EPC via a pneumatic tether and it is controlled using an array of microcompressors and valves carried by the hard robot. A wireless camera, capable of two axes of rotation, is mounted on the hard robot; it communicates with the remote computer via a WiFi link.

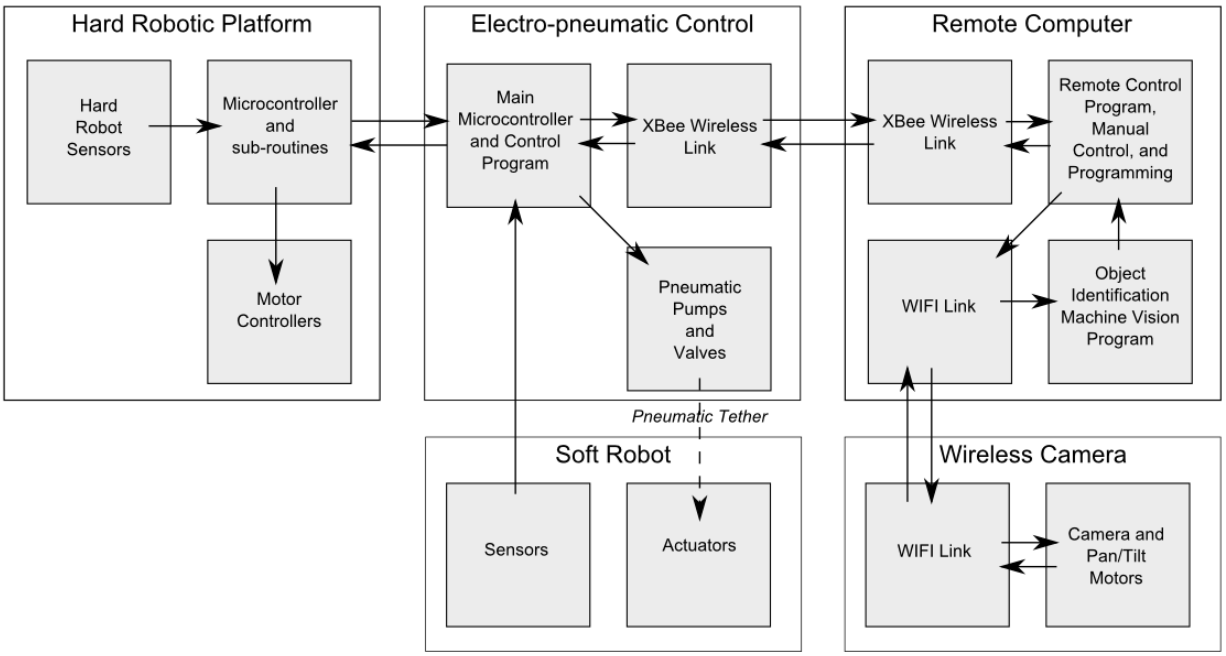
Hard Robotic Platform
Hard Robot Sensors
Microcontroller and sub-routines
Motor Controllers
Electro-pneumatic Control
Main Microcontroller and Control Program
XBee Wireless Link
Pneumatic Pumps and Valves
Remote Computer
XBee Wireless Link
Remote Control Program, Manual Control, and Programming
WIFI Link
Object Identification Machine Vision Program
Pneumatic Tether
Soft Robot
Sensors
Actuators
Wireless Camera
WIFI Link
Camera and Pan/Tilt Motors

Figure S2. A technical schematic of the ecoflex body plan of the quadrupedal robot. Dimensions are in millimeters.

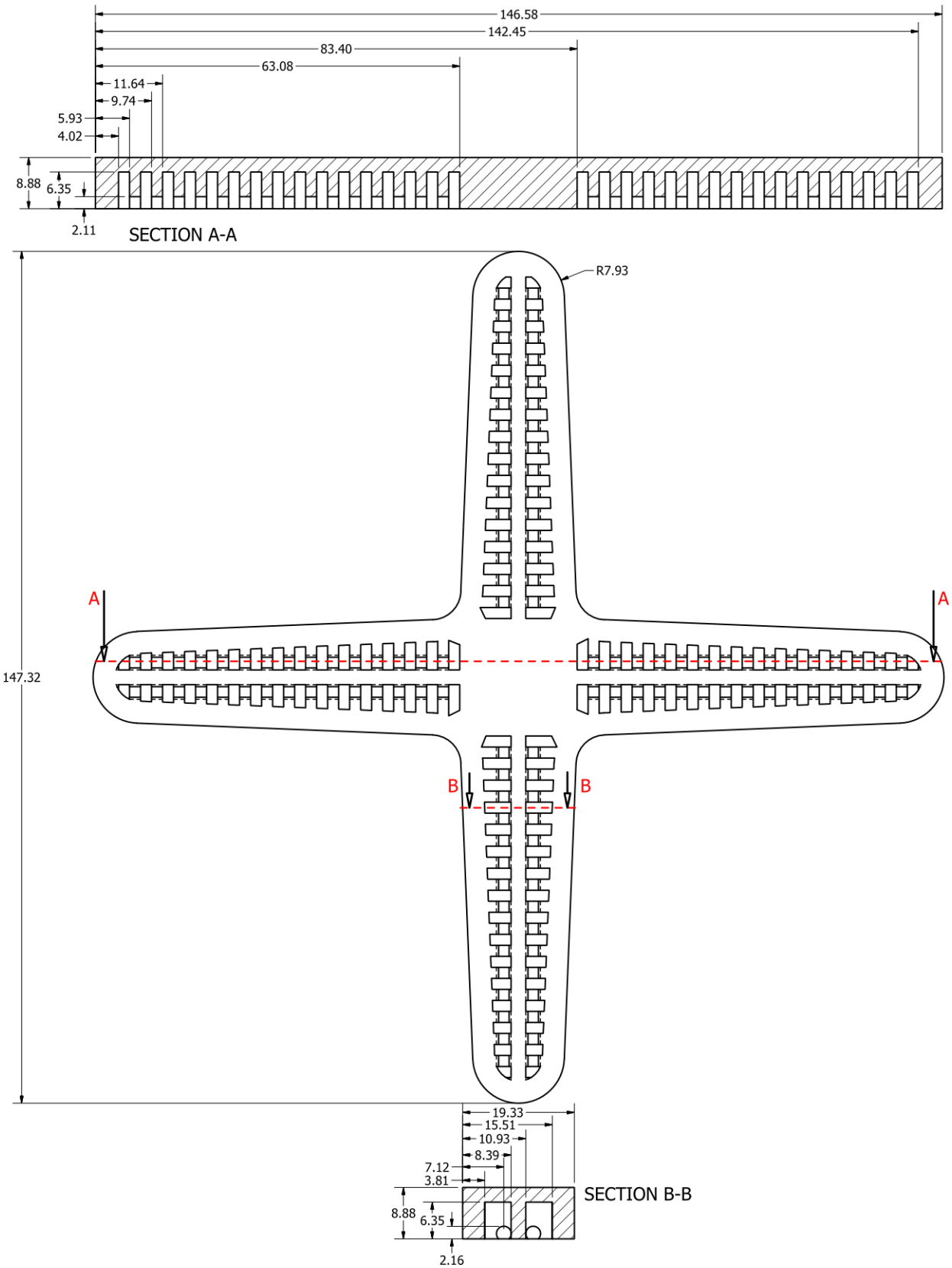
146.58
142.45
83.40
63.08
11.64
9.74
5.93
4.02
8.88
6.35
2.11
SECTION A-A
R7.93
A
A
147.32
B
B
19.33
15.51
10.93
8.39
7.12
3.81
8.88
6.35
2.16
SECTION B-B

Figure S3. A sequence of photographs demonstrating the paddling motion of one of the robot's legs. Pneu-nets are labeled PN for clarity. a) pneu-net 1 and pneu-net 2 are initially at atmospheric pressure. b) pneu-net 1 is inflated to 5 psi, the tip of the leg moves forward-and-down. c) pneu-net 1 and pneu-net 2 are inflated, the leg moves down-and-back. d) pneu-net 1 is deflated, the leg moves back-and-up. The sequence then repeats, pneu-net 1 and pneu-net 2 are deflated, and the leg returns to the position shown in a).

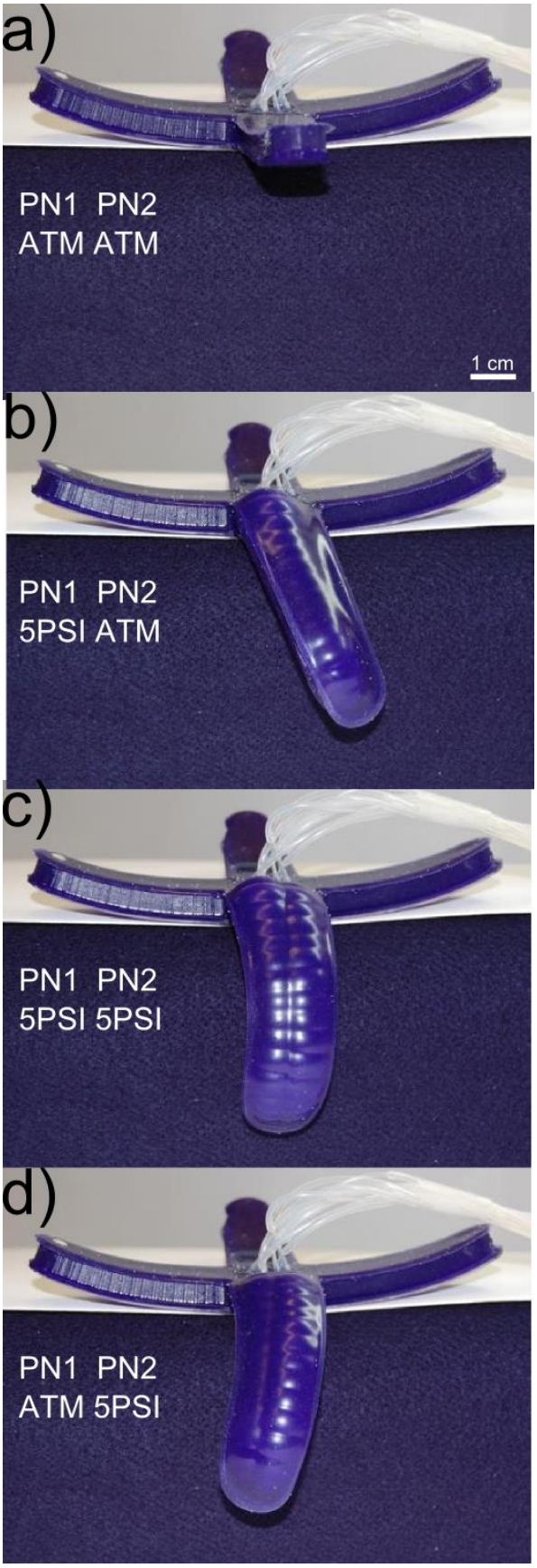
a)
PN1 PN2
ATM ATM
1 cm
b)
PN1 PN2
5PSI ATM
c)
PN1 PN2
5PSI 5PSI
d)
PN1 PN2
ATM 5PSI

Figure S4. Programming the microcontroller to direct the robot along a clockwise square path. This figure shows a composite image of four still-frames from Video S1. The robot starts in the lower left corner of the figure at t=0 s; snapshots show the robot as it walks to the upper left, upper right, and then lower right of the frame; at t=50 s, 102 s, and 158 s respectively. The colored stars correspond to the initial orientation of the robot: left hind, left fore, right fore and right hind are colored in red, green, blue, and black respectively. These stars were applied to the image (they were not physically on the robot) and were added to help in orienting the robot. The effective front of the robot is controlled by the pneu-nets actuated by the microcontroller; the quadruped does not physically turn.

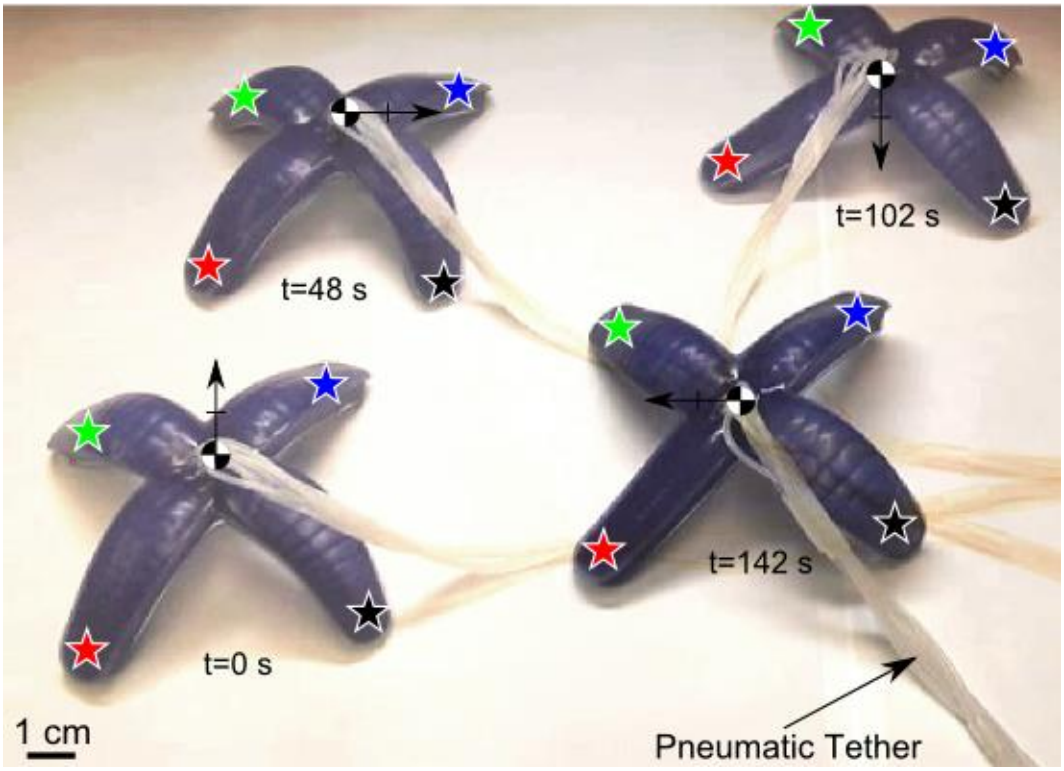
t=48 s
t=102 s
t=0 s
t=142 s
1 cm
Pneumatic Tether

Figure S5. Motion tracking data from Video S3. a) Y position of the centre of mass of the robot with respect to the origin (upper left of the video frame). The calculated Y direction velocities are -0.2, -0.03, 0.16, and -0.01 cm/s. b) X position of the centre of mass of the robot. The calculated X direction velocities are 0.03, 0.17, -0.05, and -0.18 cm/s. The combined X and Y velocities correspond to total speeds of 7.15, 6.34, 5.90, and 6.65 m/h. The average speed of the robot in any direction is, therefore, 6.51 m/h or 62 body lengths per hour.

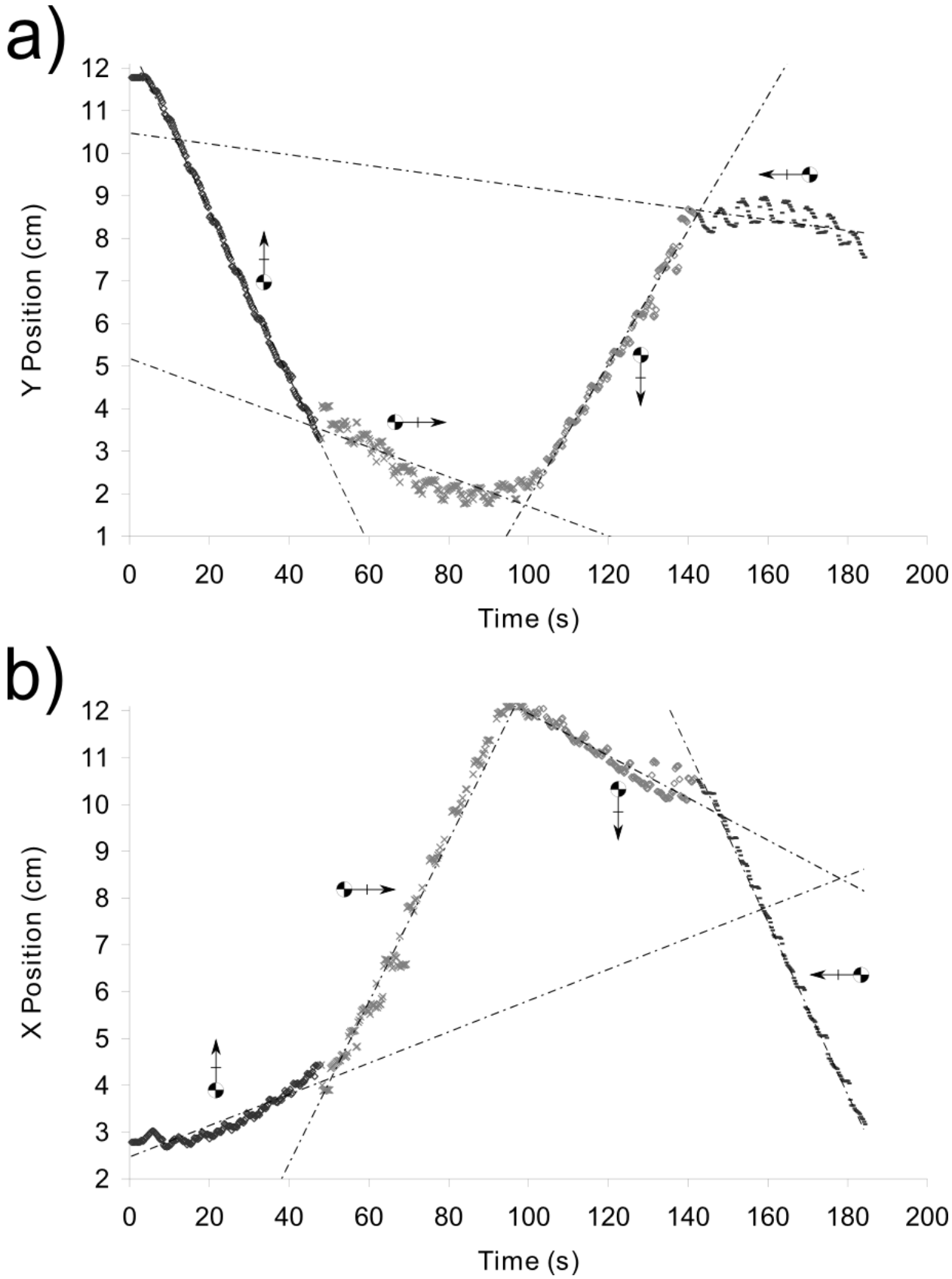
a)
Y Position (cm)
Time (s)
b)
X Position (cm)
Time (s)

Figure S6. a) This diagram shows the timing of switching, on and off, of the pumps and valves that results in motion of the robot along the RF-LF axis. b) By rotating the timing diagram it is possible to redefine which side of the robot becomes the effective front of the robot. We have split the timing diagram into nine time sections and so we use mode-9 matrix rotations. For example, a rotation of two means that the timing diagram is shifted two units to the left. The leftmost two elements would “rotate” and re-join the matrix on the right-hand side. Shown here are the leftward-matrix rotations that result in four directions of locomotion without changing the physical orientation of the soft robot.

a)

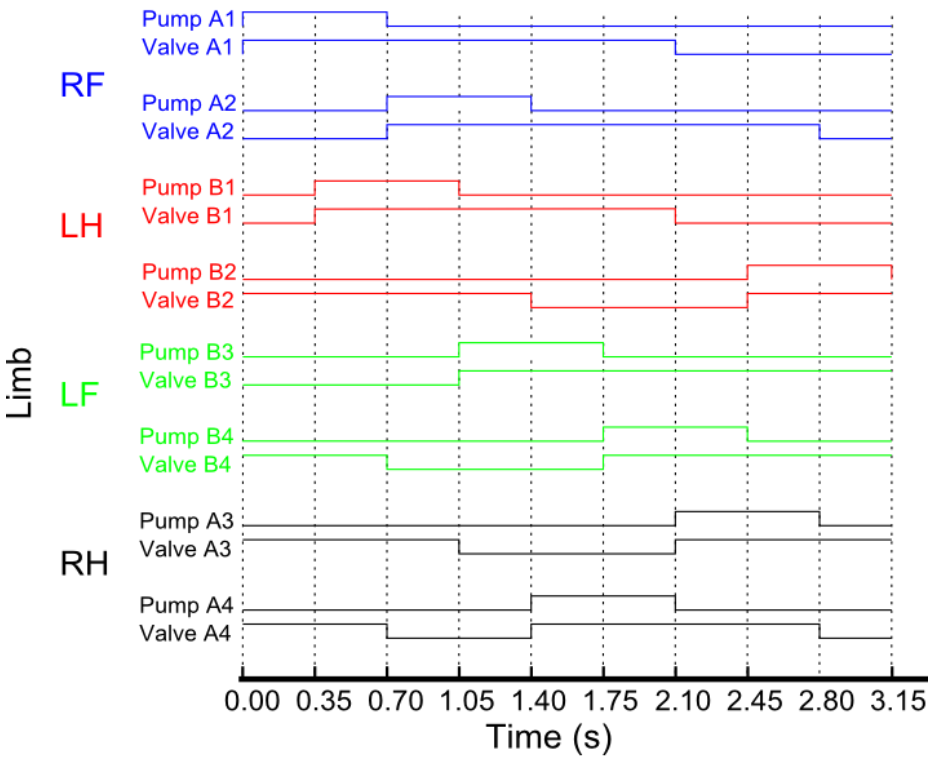

b)

Timing Diagram Rotations

Walking Direction

Limb		↑	→	↓	←
LF	Pump A1 Valve A1	**9-0 = 9**	9-3 = 6	9-1 = 8	9-6 = 3
	Pump A2 Valve A2	9-2 = 7	9-5 = 4	9-7 = 2	9-7 = 5
RH	Pump B1 Valve B1	9-1 = 8	9-6 = 3	**9-0 = 9**	9-3 = 6
	Pump B2 Valve B2	9-7 = 2	9-4 = 5	9-2 = 7	9-5 = 4
RF	Pump B3 Valve B3	9-3 = 6	9-1 = 8	9-6 = 3	**9-0 = 9**
	Pump B4 Valve B4	9-5 = 4	9-7 = 2	9-4 = 5	9-2 = 7
LH	Pump A3 Valve A3	9-6 = 3	**9-0 = 9**	9-3 = 6	9-1 = 8
	Pump A4 Valve A4	9-4 = 5	9-2 = 7	9-5 = 4	9-7 = 2

Figure S7. a) A still-frame from Video S5, showing the robot at the maximum angle of incline (~15°) that it can navigate before losing traction. The surface is paper. b) A still-frame from Video S2 showing the robot navigating an unstable granular terrain: sand.

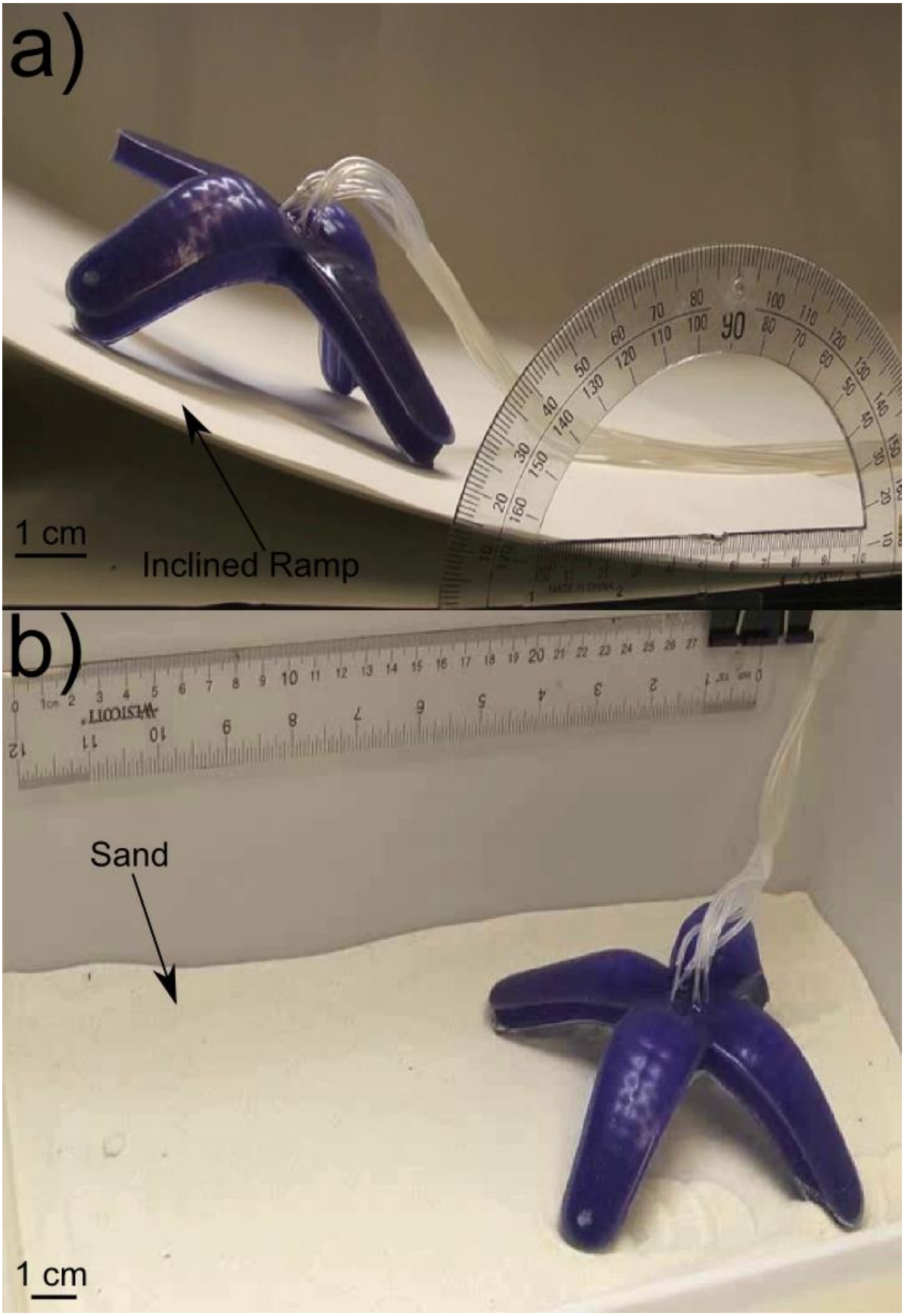
a)
1 cm
Inclined Ramp
b)
Sand
1 cm

Figure S8. Motion tracking data from Video S5. a) Y position of the centre of mass of the robot with respect to the origin (upper left of the video frame). The calculated Y direction velocity is -0.14 cm/s. b) X position of the centre of mass of the robot. The calculated X direction velocity is 0.01 cm/s. The combined X and Y velocities, for the robot walking on sand, correspond to a total speed 5.0 m/h or 48 body lengths per hour.

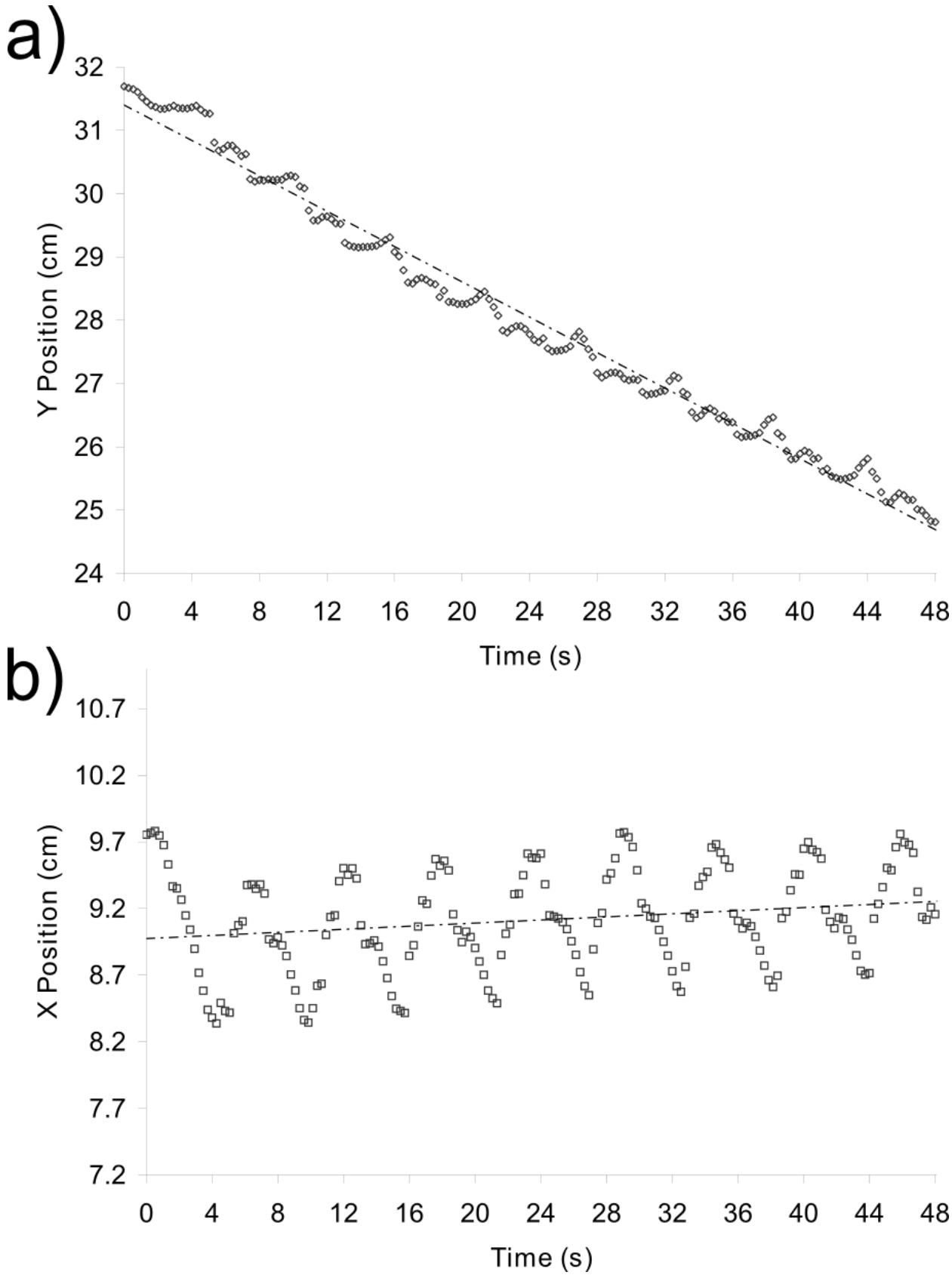
a)
Y Position (cm)
32
31
30
29
28
27
26
25
24
0
4
8
12
16
20
24
28
32
36
40
44
48
Time (s)
b)
X Position (cm)
10.7
10.2
9.7
9.2
8.7
8.2
7.7
7.2
0
4
8
12
16
20
24
28
32
36
40
44
48
Time (s)

Figure S9. A series of still frames from Video S2 shows the legged robot gripping a light bulb. a) The legs are first unactuated and then b) all legs are pressured to grip the light bulb. To show the light bulb remains undamaged, c) the legs are depressurized and the light bulb is released. The tubes corresponding to the tether exit the robotic gripper/walker at the top.

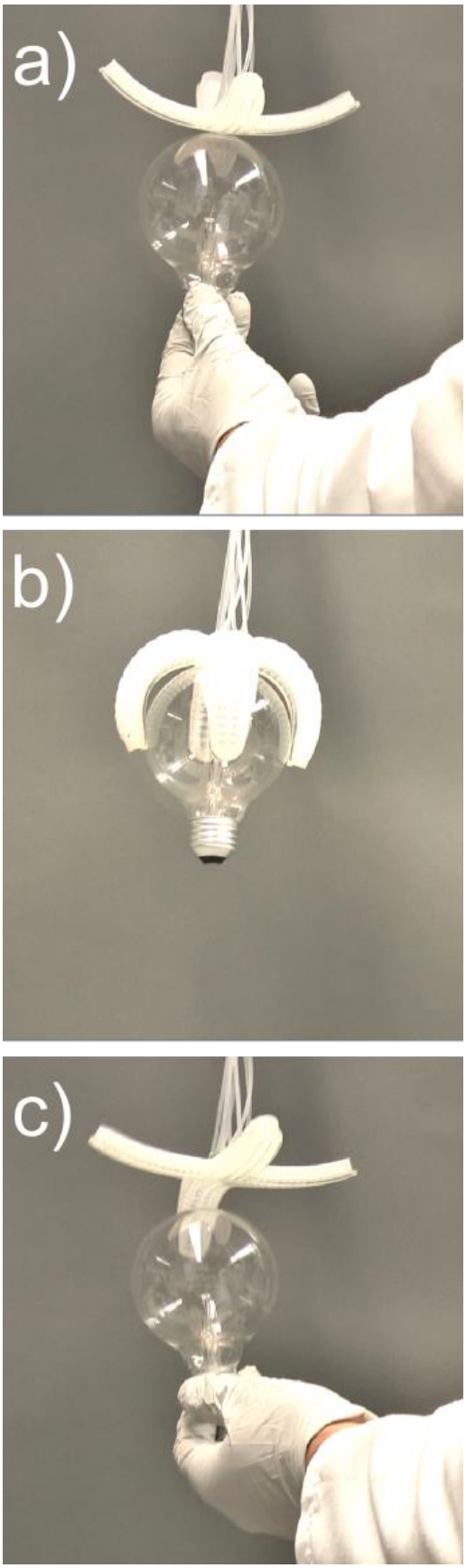
a)
b)
c)

Figure S10. a) Design of the net for the paper-MEMS based bump sensors. Stencil-printed carbon ink patches are used as piezoresistive sensors. Copper wires (not shown) are connected to the sensor using silver epoxy. b) The folded form of the sensor network showing the triangular cross section of the arm and the top-side of the flexible hinge containing the piezo sensor. c) Photograph of the soft robot with the sensor array mounted on the underside. Both the sensor network and the robot measure 15 cm from point to point through their centers.

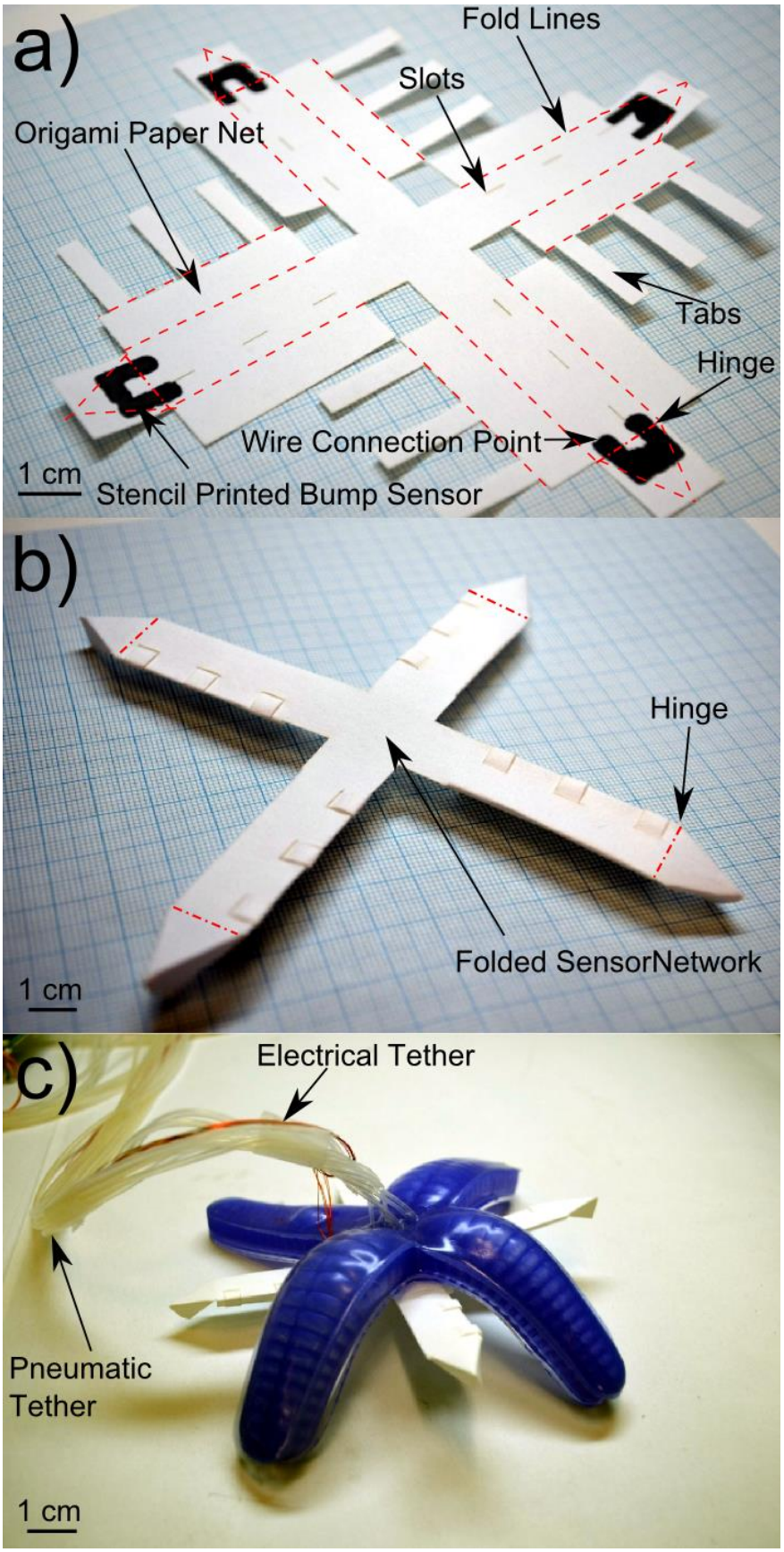
a)
Fold Lines
Slots
Origami Paper Net
Tabs
Hinge
Wire Connection Point
1 cm
Stencil Printed Bump Sensor
b)
Hinge
Folded SensorNetwork
1 cm
c)
Electrical Tether
Pneumatic
Tether
1 cm